Hypersonic Magnetohydrodynamics with or without a Blunt Body

R. H. LEVY,* P. J. GIERASCH,† AND D. B. HENDERSON‡
Avco-Everett Research Laboratory, Everett, Mass.

We consider the hypersonic flow of a cold gas past an axially symmetric body containing a magnetic dipole with its axis oriented parallel to the flow. The magnetic moment of the dipole and the size of the body are of arbitrary proportions. A uniform scalar conductivity σ is turned on by the shock, and the magnetic Reynolds number is low. We introduce an interaction parameter $S = \epsilon\sigma B_0^2 r_c/\rho_\infty u_\infty$, where $\epsilon(\ll 1)$ is the reciprocal compression ratio across a strong shock, B_0 is the magnetic field strength at the shock, r_c is the shock radius of curvature, and ρ_∞ and u_∞ are the density and velocity in the freestream. When $S \ll \epsilon^{1/2}$, the flow is quasi-aerodynamic. Certain discrepancies existing in the literature on the flow in this regime are reconciled. When $S \gg \epsilon^{1/2}$, a thin layer somewhat akin to a shock layer is formed behind the shock, but this whole layer is separated from the body by an extensive region of low Mach number flow. When $S \approx 1.6$, the entire flow field can be supported by the magnet, i.e., without the hot gas touching the body. Assuming a large compression ratio across the shock, a simple analysis can be performed. Calculations covering various representative cases are exhibited; the validity and significance of these calculations are discussed.

Nomenclature

$x, y, r, \theta,$ $R, \phi, n, s,$ $\tilde{r}, \tilde{n}, \xi$	=	various coordinates
u, v	=	velocity components
p	=	pressure
ρ	=	density
B	=	magnetic field
B_r, B_θ, B_s, B_n	=	various magnetic field components
j	=	current density
σ	=	conductivity
ψ	=	stream function
S	=	interaction parameter
ϵ	=	limiting shock compression ratio
$r_c, r_s, r_b, \Delta, \delta$	=	various distances
κ	=	curvature
k	=	reference pressure gradient
η	=	magnetic field line parameter
I, M, P	=	integral quantities
t	=	dummy variable
G, h, f_1, f_2	=	auxiliary functions

Subscripts

0	=	reference quantity
∞	=	freestream value
M	=	matching
L	=	deceleration layer

I. Introduction

WE consider the interaction between a hypersonic flow and a fixed magnetic field under conditions for which the magnetic Reynolds number is negligibly low. Such flows can be regarded as entirely aerodynamic in structure, although differing from traditional types of aerodynamic flows in that the applied forces act through a volume rather than at surfaces. In addition to assuming that the magnetic Reynolds number will be small, we shall suppose that the conductivity of our gas will be "turned on" by a strong bow shock wave. This assumption corresponds to the conditions encountered in hypersonic flight in planetary atmospheres. We shall see later on that it will be legitimate to consider this conductivity as a constant over an interesting part of the flow field. Now these general conditions have formed the basis of quite a few studies. We can distinguish two groups of such studies, namely, those in which the flow is considered to be primarily aerodynamic and is modified by the magnetic field, and those in which the flow is dominated by the magnetic interaction and the presence of a body is of secondary importance. We shall be concerned with both categories, but will emphasize in particular those flows in which forces exerted at solid surfaces play a negligible role. However, it will be useful to review briefly both categories of studies in order to establish a perspective.

A group of papers by Kemp,[1] Bush,[2] and Lykoudis[3] deals with the modification by a magnetic field of the hypersonic flow of gas over a body. The points of difference between these papers are largely in the choice of method, the actual problem being similar in all cases. Although not explicitly stated in all the papers, the general idea is that the magnetic forces are less than those exerted at the surface of the body. Bush, however, does suggest the possibility of the opposite extreme. The results of all these papers are given in terms of calculated modifications of the aerodynamic flow. Thus, the effect of the magnetic field is to reduce the stagnation-point velocity gradient, to increase the shock standoff distance, and therefore to reduce the convective stagnation-point heat transfer. The drag is largely unaffected.

A different approach is given in a paper of Levy and Petschek.[4] Here, a rather special two-dimensional problem is studied with a view to describing a flow in which the body is entirely absent. The results of such a study clearly cannot be stated with reference to any standard aerodynamic flow. Rather, such parameters as the location of the shock are given in terms, for instance, of the current flowing in the magnet. An important feature of this type of flow is the existence of an inner boundary to the flow behind which the gas density is very low. If the body that houses the magnet is inside this inner zone, it is essentially not in contact with the flow at all, and the convective heat transfer to it should be very small.

In the present paper, we attempt to combine features of both the foregoing problems. The geometry we study is

Received February 14, 1964; revision received June 17, 1964. This research was supported by Headquarters, NASA, under Contract No. NAS w-748. The authors wish to express appreciation to H. E. Petschek for helpful suggestions during the course of this work.

* Principal Research Scientist. Associate Fellow Member AIAA.
† Assistant Scientist.
‡ Assistant Engineer.

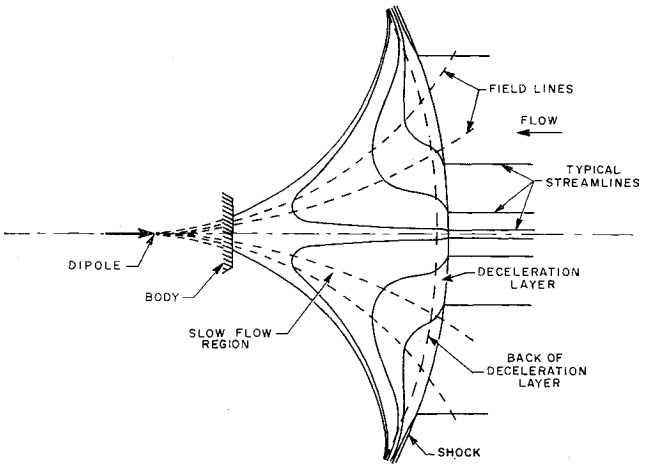

Fig. 1 Illustration of the principal features of the flow to be expected when $S \approx 1$. The conductivity is zero ahead of the shock.

the physically realistic geometry of the first group of papers, but we use the methods of Levy and Petschek and concentrate strongly on the case in which the body plays a negligible role in the flow. In the course of the work, certain discrepancies existing in the first group of papers are resolved, and the flow corresponding to the limit discussed by Bush is extensively described. In subsequent sections, we will analyze the flow in greater detail and discuss particularly the limiting cases in which the flow is principally supported by either the magnetic field or the body. In the last section, we will draw some general conclusions from our study and also describe some of the physical limitations on the validity of our analysis.

The entire analysis described in this paper has been extended to the corresponding two-dimensional problems by Levy et al.[5]; this reference also treats the subject matter of this paper at greater length.

II. Description and Analysis of the Flow

The general features of the flow to be treated are illustrated in Fig. 1, and the coordinate systems and other dimensions used in the analysis are shown in Fig. 2. A strong shock is formed in the gas ahead of the object; behind this shock the gas is weakly conducting. We neglect heat conduction and

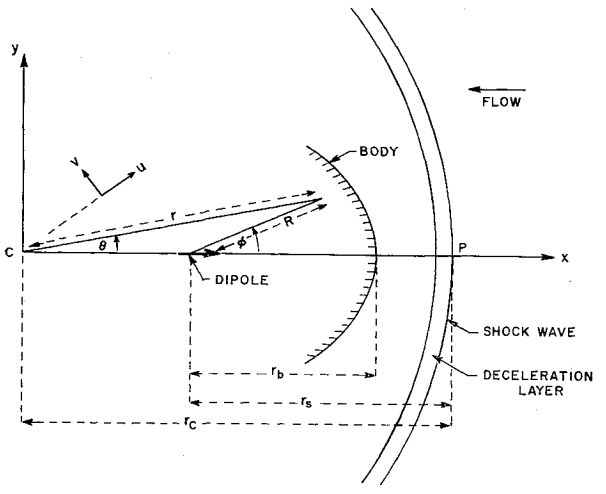

Fig. 2 Illustration of the coordinate systems used in the text. C is the center of curvature of the deceleration layer at the point P. The components (u,v) of the velocity are polar and are referred to the coordinate system (r, θ) with origin at C.

viscosity since the viscous Reynolds number is high; when there is no body in the flow there will not even be a thin viscous boundary layer. The current flow (in the absence of Hall effect) is in the azimuthal direction, and it follows that $\mathbf{j}\cdot\mathbf{E} = 0$. Thus, in our case, each streamline is isolated energetically and therefore has a constant total enthalpy. It follows that the total enthalpy is constant throughout the flow and equal, since the flow is hypersonic, to $\frac{1}{2}u_\infty^2$. In the region where the Mach number is low (behind the normal part of the shock, for example), the static enthalpy will be approximately constant. We shall assume that the properties of the gas are such that the electrical conductivity may be treated as constant when the enthalpy is constant, even though the gas may undergo a considerable expansion. This assumption will allow us to take the conductivity as constant through a large part of the flow. We also assume that the gas conditions are such that the Hall effect may be neglected; in the last section we shall estimate limits to the validity of this assumption.

The statement that the gas is weakly conducting behind the shock is to be taken to mean that the magnetic Reynolds number is low. The general features of flows at low magnetic Reynolds numbers have been outlined elsewhere.[6,7] In order to have a substantial exchange of momentum between the field and the flow, the product of the magnetic Reynolds number and the ratio of magnetic to dynamic pressures must be of order unity. We call this product the interaction parameter and denote it by S. Throughout this paper, we will use an interaction parameter defined by $S = \epsilon\sigma B_0^2 r_c/\rho_\infty u_\infty$, where $\epsilon(\ll 1)$ is the reciprocal compression ratio across the shock, σ the conductivity behind the shock, B_0 the field strength at the normal point of the shock, and r_c the radius of curvature of the shock.

The geometrical configuration shown in Fig. 1 is generically the same as that treated by Bush et al. The body is taken to be axially symmetric but need not be spherical. The magnetic field is that due to a dipole whose axis coincides with the axis of the body and with the flow direction. The location of the dipole is, within the limitations of symmetry, arbitrary, except that it is supposed not to be right at the stagnation point of the body. Also, we do not make any a priori assumption about the shape or the location of the shock.

We define the deceleration layer (Fig. 1) as the region just behind the shock for which the velocity component parallel to the shock is larger than the component normal to the shock. (The deceleration layer reduces when there is no magnetic interaction to the aerodynamic shock layer. The reason for this choice of terminology will become apparent later on.) Although this definition breaks down near the place where the shock is normal, it can be extended in a consistent manner to the stagnation streamline by using the gradient of the velocity component parallel to the shock, multiplied by the radius of curvature of the shock. The important thing to notice is that, because of the requirement of continuity, the deceleration layer as defined is thin. In fact, since the ratio of the velocity components perpendicular and parallel to the shock is on the order of ϵ, the continuity equation tells us that the thickness of the layer is approximately ϵr_c, where r_c is the radius of curvature of the shock. Since $\epsilon \ll 1$, we introduce in the deceleration layer the expanded coordinate $\bar{r}$ defined by $\bar{r} = \epsilon^{-1}(1 - r/r_c)$, so that $\bar{r} = 0$ at the shock and is of order unity at the back of the layer.

We commence our detailed analysis of the flow problem in that part of the deceleration layer which is close to the place where the shock is normal. We nondimensionalize all the flow quantities in accordance with the general picture of the flow anticipated in the deceleration layer. Thus, the pressure is nondimensionalized with the freestream dynamic pressure, $\rho_\infty u_\infty^2$, the density with the density behind a strong shock, ρ_∞/ϵ, all distances with r_c, the velocity components in the radial and tangential directions with ϵu_∞ and u_∞, and

the magnetic field with B_0. In the deceleration layer we shall neglect $1/r$ compared with $\partial/\partial r = (-1/\epsilon r_s)(\partial/\partial\tilde{r})$. We also neglect the change in the field components across the layer.

The energy equation, as has already been explained, has for an integral the condition of constant total enthalpy throughout the flow. We shall suppose the gas to be so close to perfect that the enthalpy may be taken to be proportional to p/ρ. Then, with the nondimensionalization just described, the energy equation reduces to

$$p = \rho(1 - v^2) \tag{2.1}$$

with the neglect of terms of order ϵ^2. v, B_θ, and j are odd functions of θ, and all other quantities are even functions of θ. Hence, on the stagnation streamline $\theta = 0$,

$$p = \rho \tag{2.2}$$

The equation of continuity reduces, on the stagnation streamline, to

$$d(\rho u)/d\tilde{r} = 2\rho\, \partial v/\partial\theta \tag{2.3}$$

The quantities appearing in (2.2) and (2.3) are regarded as functions of $\tilde{r}$ only. This method gives the appearance of treating the stagnation streamline by itself, but is, in fact, no different in principle from the methods common in aerodynamics[8] involving expansions in powers of θ. On the stagnation streamline the current (nondimensionalized with $\sigma u_\infty B_0$) is given by

$$\partial j/\partial\theta = \epsilon u \partial B_\theta/\partial\theta - B_r \partial v/\partial\theta \tag{2.4}$$

This is the appropriate form of Ohm's law. We shall assume that $\partial B_\theta/\partial\theta \ll \epsilon^{-1}B_r$. This condition implies only that the dipole is not located right at the back of the deceleration layer. A result of this assumption is that we may take the current in the deceleration layer to be given on the stagnation streamline by

$$\partial j/\partial\theta = -\partial v/\partial\theta \tag{2.5}$$

The radial momentum equation reduces in the deceleration layer to

$$\rho v^2 + dp/d\tilde{r} + SB_\theta v = 0 \tag{2.6}$$

On the stagnation streamline, this gives

$$dp/d\tilde{r} = 0 \text{ and therefore } p = 1 \tag{2.7}$$

Thus, to this approximation, the pressure on the stagnation streamline is constant. From (2.2) we immediately deduce, also for the stagnation streamline, that the density is constant, or $\rho = 1$. Applying this to the continuity equation as written for the stagnation streamline (2.3) gives

$$du/d\tilde{r} = 2\,\partial v/\partial\theta \tag{2.8}$$

We shall use (2.6) to deduce the pressure gradient at the back of the deceleration layer when we have found a suitable profile for v. We therefore differentiate it twice with respect to θ and set $\theta = 0$ to find (since $\rho = 1$)

$$d(\partial^2 p/\partial\theta^2)/d\tilde{r} = -2(\partial v/\partial\theta)^2 - 2S(\partial B_\theta/\partial\theta)(\partial v/\partial\theta) \tag{2.9}$$

We shall return to this equation in due course. The tangential momentum equation in the deceleration layer reduces on the stagnation streamline (after differentiation with respect to θ) to

$$-ud(\partial v/\partial\theta)/d\tilde{r} + (\partial v/\partial\theta)^2 + \epsilon\partial^2 p/\partial\theta^2 + S\partial v/\partial\theta = 0 \tag{2.10}$$

We can neglect the pressure gradient in this equation as long as we do not integrate beyond the point where the other terms become comparable to the pressure gradient. Thus,

$$-ud(\partial v/\partial\theta)/d\tilde{r} + (\partial v/\partial\theta)^2 + S\partial v/\partial\theta = 0 \tag{2.11}$$

This must be solved, together with (2.8). The boundary conditions at the shock are $u = -1$, $\partial v/\partial\theta = 1$. The solution may be written implicity as

$$\tilde{r} = \{[1 - (-u)^{1/2}]/(1 + S)\} - [S/(1 + S)^2]\ln[(-u)^{1/2}(1 + S) - S] \tag{2.12}$$

$$\tilde{r} = [(1 - \partial v/\partial\theta) - S\ln\partial v/\partial\theta](1 + S)^{-2}$$

These equations show the principal features of the behavior of the flow in the deceleration layer. The inward radial velocity tends to the limit $S^2/(1 + S)^2$, whereas the tangential velocity decreases without limit as we approach the back of the layer. In order to find the back of the deceleration layer, we use the profile of (2.12) in (2.10) and see at what point the equation is no longer a balance between two terms both larger than the pressure gradient term. Substitution shows that we must distinguish two cases:

1) If S is small, (2.10) can be considered as a balance between the two convective terms. This is the aerodynamic limit. At a distance $\tilde{r} \approx 1$, $\partial v/\partial\theta \approx \epsilon^{1/2}$, and the pressure gradient becomes important. At this point $-u \approx \epsilon$.

2) If S is large, (2.10) can be considered as a balance between the first of the two convective terms and the magnetic term. This is the magnetohydrodynamic limit. At a distance $\tilde{r} = S(1 + S)^{-2}\ln(S/\epsilon)$, $S(\partial v/\partial\theta) = \epsilon$, and the pressure gradient becomes important. At this point $-u = S^2(1 + S)^{-2}$.

This leads to an interesting situation; apart from extremely small values of the interaction parameter, the transverse component of the velocity at some distance back from the shock may fall to low values before we reach the body (the body is where the radial velocity vanishes). By our definition, the place where the two components are comparable in magnitude is the back of the deceleration layer. Thus, in the magnetohydrodynamic case, there may be an outflow from the back of the deceleration layer. There is, therefore, an additional flow region behind the deceleration layer which will have to be studied in order to complete the solution to the whole flow problem. In view of the fact that in this region both velocity components are of order ϵu_∞, we call it the "slow flow region" (see Fig. 1). Since the Mach number is very low, the convection of momentum in it will be negligible compared to the pressure gradients and the magnetohydrodynamic forces. The balance of these last two, therefore, determines the nature of the flow. Two additional remarks concerning the slow flow region are important. First, since the velocity components in both directions are comparable, the equation of continuity shows that the dimensions of the slow flow region are roughly comparable in all directions. Secondly, since there is no magnetohydrodynamic force along the field lines, the pressure is a given constant for each field line.

Now, in order to solve the flow in the slow flow region, we must know, from study of the deceleration layer, the pressure on each field line and the flow velocity across the boundary between the regions. We have shown how to calculate the latter, and it remains to determine the pressure at the back of the layer. This is done using (2.9). Now $\partial^2 p/\partial\theta^2 = -2$ at the shock, $\tilde{r} = 0$, since $p \sim \cos^2\theta$. Therefore, integrating (2.9) and evaluating it at the back of the deceleration layer where $\partial v/\partial\theta$ is small, we find

$$k = -\frac{\partial^2 p}{\partial\theta^2}\bigg|_{\substack{\theta = 0 \\ \tilde{r} = \infty}} = 2 + \frac{2/3}{(1 + S)^2} + \frac{S[1 + (\partial B_\theta/\partial\theta)]}{(1 + S)^2} + \frac{2S^2(\partial B_\theta/\partial\theta)}{(1 + S)^2} \tag{2.13}$$

The first of these terms represents the pressure gradient at the shock, the second is the centrifugal effect, and the last two are the magnetohydrodynamic effect. For the dipole, as shown in Fig. 2,

$$\partial B_\theta/\partial\theta|_{\text{stag. pt.}} = (3 - 2r_s)/2r_s \tag{2.14}$$

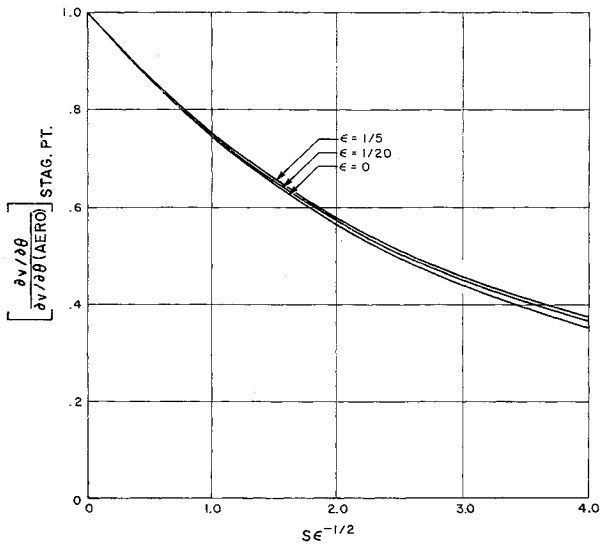

Fig. 3 Illustration of the reduction in the stagnation-point velocity gradient effected by introducing a magnetic field. The calculation is reasonable only as far as $S\epsilon^{-1/2} \approx 1$.

If the dipole happens to be right at the center of curvature of the shock, $r_s = 1$. We see that the centrifugal effect is always weakened by the presence of a magnetic field and that the magnetohydrodynamic effect can be of either sign, depending on whether the field lines in the deceleration layer appear to diverge from a point ahead of or behind the center of curvature of the deceleration layer. These remarks explain the difference in the sign of the change in the body pressure gradient in the work of Kemp and Bush. Kemp has a pole at the center of curvature of the deceleration layer. The only effect on the pressure is, then, that the centrifugal effect is reduced. As a result, the pressure at the body is higher than in the aerodynamic case, and the stagnation-point pressure gradient is reduced. Bush, on the other hand, has a dipole at the center of curvature of the shock layer. Thus, the magnetic force is outward, the pressure on the body is reduced, and the stagnation-point pressure gradient is increased.

In order to find the remaining details of the deceleration layer near $\theta = 0$, we substitute k for the pressure gradient in (2.10). This will not affect the solution near the front of the layer (where $-\partial p^2/\partial\theta^2 = -2$ not k) but is important at the back, where $\partial^2 p/\partial\theta^2$ is equal to k. Equation (2.10) becomes

$$-ud(\partial v/\partial\theta)/d\tilde{r} + (\partial v/\partial\theta)^2 + S\partial v/\partial\theta - k\epsilon = 0 \quad (2.15)$$

Equations (2.8) and (2.15) have been integrated by Lykoudis[3] on the assumption that $k = \frac{8}{3}$, its aerodynamic value, obtained from (2.13) by setting $S = 0$. We have repeated the integration using (2.13) as appropriate. The stagnation-point velocity gradient ratio is plotted in Fig. 3. The standoff distance is plotted in Fig. 4. The differences from Lykoudis' calculation are small when $S\epsilon^{-1/2}$ is small. The line on Fig. 3 marked $\epsilon = 0$ corresponds exactly to Lykoudis' calculation in the sense that if $\epsilon = 0$, but $S\epsilon^{-1/2}$ is finite, S must be zero and hence k takes its aerodynamic value. Also shown in Fig. 4 are the thicknesses of the deceleration layer, defined as the region where $1 \geq -u \geq S^2(1 + S)^{-2}$. The difference between these two lengths is the incipient slow flow region. All the lengths in Fig. 4 are normalized with respect to the aerodynamic standoff distance, $\epsilon[1 + (8\epsilon/3)^{1/2}]^{-1}$. It can be seen that, with increasing $S\epsilon^{-1/2}$, the deceleration layer thickness does not change very much, whereas the total standoff distance grows rapidly. This merely confirms our previous discussion in which, for large $S\epsilon^{-1/2}$ we divided the flow into a thin deceleration layer and a fat slow flow region. Figure 4, therefore, illustrates the incipient growth of the slow flow region. It cannot, however, be used, as Lykoudis has used it, to determine the distance between the body and the shock when $S\epsilon^{-1/2} >$ about 1. The reasons for this are that the assumptions that went into (2.15) from which the numbers appearing in Fig. 4 were calculated are violated as follows in the region $-u < S^2(1 + S)^{-2}$.

1) The tangential velocity is reduced to the same order of magnitude as the radial velocity, so that, referring to (2.4), the current is no longer given by (2.5).

2) The fact that the velocity components are equal in order of magnitude implies that the scale of the problem is no longer compressed. Thus, the flow now extends over regions comparable in size in all directions with the body, and the pressure gradient can no longer be treated as constant.

3) The deceleration layer can no longer be assumed concentric with the body and the dipole.

To conclude this part of the work, we point out that the type of analysis used here, in the magnetohydrodynamic as in the aerodynamic case, gives the standoff distance of the shock in terms of the shock radius of curvature, but does not give the radius of curvature of the body. To establish the body radius of curvature, we must consider the flow at greater distances from the stagnation streamline.

We next turn to the study of the slow flow region, which intervenes between the deceleration layer and the body and in which both velocity components are of order ϵu_∞. Since this velocity is strongly subsonic, the enthalpy is effectively constant and from (2.1),

$$p = \rho \quad (2.16)$$

although these quantities will vary considerably through the region. We note that this isenthalpic motion may involve a considerable rise in the entropy. Since the flow is subsonic, we may neglect the convection of momentum and consider the flow to be governed by the remains of the momentum equation:

$$\nabla p = S\mathbf{j} \times \mathbf{B} \quad (2.17)$$

The neglect of the inertia term in (2.17) will result in infinite velocities; these should be interpreted as sonic. The equation of continuity is

$$\nabla \cdot \rho\mathbf{u} = 0 \quad (2.18)$$

These equations may be considered to have been nondimensionalized just as before, with two exceptions. Both components of velocity are now nondimensionalized with respect to ϵu_∞, and distances are referred simply to r_c. The current now involves contributions from both velocity components. We shall find it convenient to work in the polar coordinates (R,ϕ) fixed at the dipole and define the radial and tangential velocity components in these coordinates by means of a stream function ψ, nondimensionalized with respect to $\rho_\infty u_\infty r_c$. The components are

$$-\frac{1}{\rho R \sin\phi}\frac{\partial}{\partial\phi}(\psi \sin\phi) \qquad \frac{1}{\rho R}\frac{\partial}{\partial R}(\psi R) \quad (2.19)$$

Note that this stream function is defined like a vector potential, that is to say, the mass flow vector is represented as the curl of a vector of magnitude ψ pointing in the azimuthal direction. Thus, the streamlines are represented not by $\psi = \text{const}$, but by $R \sin\phi\psi = \text{const}$. The choice of definition is arbitrary, but the distinction must be remembered when plotting streamlines. We multiply (2.17) by $p = \rho$ and find

$$\tfrac{1}{2}\nabla p^2 = S(\rho\mathbf{v} \times \mathbf{B}) \times \mathbf{B} \quad (2.20)$$

When we substitute from (2.19) in (2.20), we find two linear equations [the components of (2.20)] for the two unknowns p^2 and ψ. The field components are

$$\mathbf{B} = (r_s/R)^3 \cos\phi \qquad \tfrac{1}{2}(r_s/R)^3 \sin\phi \quad (2.21)$$

Resolution of (2.20) along the magnetic field gives the result that p is a function only of

$$\eta = r_s^2 R^{-1} \sin^2\phi \tag{2.22}$$

so that the pressure has a constant value on any field line. Resolution of (2.20) across the field lines and use of the knowledge that $p = p(\eta)$ lead to

$$-\sin\phi \frac{dp^2}{d\eta} = S\left(\frac{r_s}{R}\right)^4 \left[\frac{\cos\phi}{R}\frac{\partial}{\partial R}(R\psi) + \frac{1}{2R}\frac{\partial}{\partial\phi}(\psi\sin\phi)\right] \tag{2.23}$$

In view of the fact that $dp^2/d\eta$, like p, is a function of η alone, we can find solutions of (2.23) of the form

$$\psi = -(1/S)(dp^2/d\eta)G(R, \phi) \tag{2.24}$$

G satisfies the equation

$$\left(\frac{r_s}{R}\right)^4 \left[\frac{\cos\phi}{R}\frac{\partial}{\partial R}(GR) + \frac{1}{2R}\frac{\partial}{\partial\phi}(G\sin\phi)\right] = \sin\phi \tag{2.25}$$

A particular solution of this equation is

$$G = \left(\frac{2R^5}{r_s^4}\right)\sin^{-13}\phi \int_0^\phi \sin^{13} t\,dt \tag{2.26}$$

In addition, any function $(R\sin\phi)^{-1} h(\eta)$ satisfies the homogeneous part of (2.25) so that the general solution of the problem is

$$\psi = -\frac{1}{S}\frac{dp^2}{d\eta}\frac{1}{Rr_s^4\sin\phi}\left[\frac{2R^6}{\sin^{12}\phi}\int_0^\phi \sin^{13} t\,dt + \eta h(\eta)\right] \tag{2.27}$$

This equation tells us everything we need to know about the slow flow region. We notice in particular that ψ vanishes on three separate lines: first, on the stagnation streamline since (by symmetry) $dp/d\eta$ vanishes; second, on the body where the quantity in brackets vanishes. Since $h(\eta)$ is arbitrary, any body can be described. Finally, ψ vanishes on the two symmetrically placed field lines for which p vanishes.

We find some relationships among S, r_s, and r_b by using the results just obtained. At the back of the deceleration layer the pressure is given for small values of θ (and therefore for small η) by

$$p \approx 1 - \tfrac{1}{2}kr_s\eta \tag{2.28}$$

from (2.13) and the definition of η (2.22). Since, in the slow flow region, p is a function of η alone, (2.28) is valid for any r between the shock and the body. Next, we specialize the general solution for the stream function in the slow flow region (2.27) to the stagnation streamline. This gives us

$$\psi \approx (r\theta k/Sr_s^3)\{(R^4/7) + [h(0)r_s^2/R^3]\} \tag{2.29}$$

From this relation, we can find the flow near $\theta = 0$ all the way from the shock to the body. In particular, at the shock we can calculate the radial velocity

$$u \approx (-1/\rho r_s\phi)\,\partial(\psi\phi)/\partial\phi \approx (-1/\theta)\partial(\psi\theta)/\partial\theta\,|_{\theta=0;\,r=1} \tag{2.30}$$

However, this radial velocity has already been calculated in (2.12). It is just the residual radial velocity at the back of the deceleration layer. Thus, we find the important matching condition

$$[S/(1+S)]^2 = (2k/Sr_s^3)\{(r_s^4/7) + [h(0)/r_s]\} \tag{2.31}$$

To find $h(0)$, we recall that the body is given when $\psi = 0$ as a result of the vanishing of the last bracket in (2.29). Using this to eliminate $h(0)$ from (2.31) gives

$$21S^3 - [18S^2 + (24r_s + 9)S + 16r_s] \times [1 - (r_b/r_s)^7] = 0 \tag{2.32}$$

This is the sought after relation between S, r_s, and r_b. From it we can make a number of deductions, the most important of which is the following: In a given flight situation (i.e., ρ_∞, u_∞, and ϵ given, as well as the magnetic moment of the dipole and its location relative to the body), (2.32) does not give unique values for the quantities appearing in it. We recall that r_b and r_s are nondimensionalized with respect to r_c, and that r_c is also the length appearing in the definition of S. Suppose some value of r_c is given; then from the geometry we can calculate r_b. However, S is proportional to B_0^2, which in turn is proportional to the inverse sixth power of r_s. But this procedure will be valid for any r_c, and there is no way of knowing which is correct.

We measure the standoff distance by means of a nondimensional distance $\Delta = (r_s/r_b) - 1$. Equation (2.32) gives, in terms of S and r_s,

$$\Delta = [1 - 21S^3\{18S^2 + (24r_s + 9)S + 16r_s\}^{-1}]^{1/7} - 1 \tag{2.33}$$

The standoff distances calculated in this way are not directly comparable to the aerodynamic standoff distance, for the aerodynamic standoff distance is a quantity of order ϵ, whereas Δ in (2.33) is of order unity. This is a result of the slow flow region having comparable dimensions parallel and perpendicular to the flow. These remarks also explain why, if we put $S = 0$ in (2.33), we recover $\Delta = 0$.

There are values of S and r_s such that $\Delta \to \infty$. They satisfy the relation

$$21S^3 - 18S^2 - (24r_s + 9)S - 16r_s = 0 \tag{2.34}$$

These values are of particular interest to us. They do not correspond to an infinite distance from the shock to the dipole, but rather to a zero distance between the body and the dipole $r_b = 0$. Thus, they correspond to what we refer to as the fully magnetohydrodynamic case. The region on the body in contact with the flow shrinks to a point, and the entire drag generated by the flow field is felt by the magnet.

We can compare our analytical calculations (for $\epsilon \ll 1$) up to this point with Bush's numerical calculations for $\epsilon = \frac{1}{11}$, which assume the dipole is at the center of curvature of the shock, by setting $r_s = 1$ in (2.33). When the interaction parameters are modified to allow for differences in notation, the agreement is quite good. In particular, for the axisymmetric case, Bush finds $\Delta = \infty$ for $S \approx 1.53$. This compares with our value $\Delta = \infty$ for $S = 1.90$ from (2.34) with

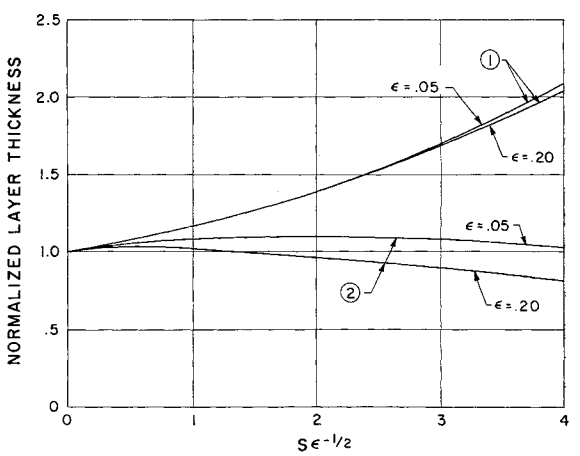

Fig. 4 Illustration of the increase in the shock standoff distance effected by introducing a magnetic field. The calculation is reasonable only as far as $S\epsilon^{-1/2} \approx 1$. The lines marked 1 represent the entire standoff distance. The lines marked 2 give the thickness of the deceleration layer defined as extending from the shock to the place where $-u = S^2(1+S)^{-2}$. These lengths are normalized with respect to the aerodynamic shock-layer thickness.

$r_s = 1$. The difference can probably be attributed to finite ϵ effects.

The picture we now have of the flow for $S \gg \epsilon^{1/2}$ is as follows. The deceleration layer is no longer in contact with the body, but is separated from it by the slow flow region. There is no longer any justification for assuming that the layer is concentric with the body, or, for that matter, with the dipole. Whatever the geometry, the type of flow we expect is illustrated schematically in Fig. 1. The pressure at the back of the deceleration layer is reduced by the combined action of the centrifugal and magnetic forces. At the same time, the component of velocity parallel to the deceleration layer at the back of the layer rises as we proceed away from the stagnation streamline; the gradient of this velocity component at the stagnation streamline is $\epsilon u_\infty r_c^{-1}$, but it will subsequently grow more rapidly when the angle between the field and the deceleration layer becomes small. At some point, it will reach sonic velocity $\epsilon^{1/2}u_\infty$. At this point, the flow in the "slow flow region" can no longer be slow. On the other hand, flow that entered the slow flow region near the axis can be expected to escape at higher speed in the general direction of the magnetic field. The analysis of this flow is beset with a number of difficulties. Thus, as the velocity rises, the temperature and hence the conductivity will fall; furthermore, the density will also be lower away from the stagnation streamline; at some point nonequilibrium, Hall and ion-slip effects must all become important. Two methods are available at this stage. The first, used by Bush (and others), is to introduce the ad hoc assumption that the dipole is at the center of curvature of the shock wave. No justification of this assumption seems possible, but it does lead to a definite problem that can be solved without discussing the tricky matter of the nature of the flow near the sonic points. The second alternative is to construct a satisfactory model of the flow out to the sonic point. In this paper we have adopted the second alternative; we shall see, however, that in order to construct this flow we are obliged to make assumptions about gas properties that are not too well justified in practice. An important result of our analysis will be a reasonable degree of agreement between our results and those of Bush. Since the results are obtained by different methods, it is felt that each lends support to the other.

We now have a solution for the slow flow region valid everywhere behind the deceleration layer and a solution for the deceleration layer near the stagnation streamline. To complete the construction of a model valid to the sonic point

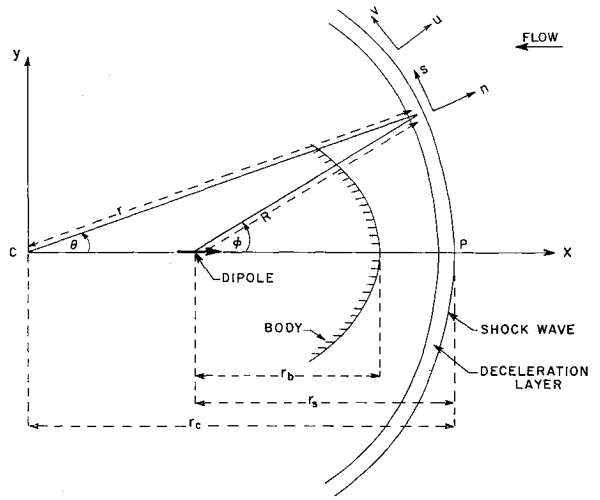

Fig. 5 Illustration of the coordinate system used in the analysis of the deceleration layer away from the stagnation line. *C* is the center of curvature of the deceleration layer at the point *P*. The components (u, v) of the velocity are, respectively, in the n and s directions. In the text, the length r_c is taken to be unity.

we need to study the deceleration layer away from the stagnation streamline. The results we need, in order to match a possible shock configuration to the slow flow region, are the pressure and the normal velocity at the back of the layer. In the absence of analytical solutions we have to resort to approximate methods. Since we do not know a priori the shape of the layer, we must introduce an arbitrary system of coordinates fixed in the layer. This system is shown in Fig. 5. n and s are coordinates perpendicular and parallel to the layer. The position of the layer itself is referred to Cartesian coordinates fixed at the center of curvature of the normal part of the layer. Thus, it is given parametrically in terms of the arc length s by $x = x_L(s)$, $y = y_L(s)$; the subscript referring to the layer. Using (as before) r_c as the unit of length, x_L and y_L are given for small s by

$$x_L = 1 - \tfrac{1}{2}s^2 \ldots \qquad y_L = s - \tfrac{1}{6}s^3 \ldots \tag{2.35}$$

u and v are the components of velocity in the n and s directions. Since the thickness of the layer is on the order of ϵr_c, we introduce a coordinate $\tilde{n}$ such that $\tilde{n} = 0$ is at the shock and $\partial/\partial\tilde{n} = (-1/\epsilon)\,\partial/\partial n$. The continuity equation is

$$\partial(\rho u)/\partial\tilde{n} - (1/y_L)\partial(\rho v y_L)/\partial s = 0 \tag{2.36}$$

where u and v are nondimensionalized with respect to ϵu_∞ and u_∞, respectively. The current is effectively given by

$$j = -vB_n \tag{2.37}$$

where B_n is the component of the magnetic field normal to the layer. This expression is valid until B_n is comparable with ϵB_s, where B_s is the component of the magnetic field parallel to the layer. At this point, as we will see, the current no longer affects the dynamics of the layer appreciably and can therefore be neglected. B_s and B_n may be regarded as functions of s only. The normal momentum equation becomes

$$\kappa\rho v^2 + \partial p/\partial\tilde{n} + Sv\,B_nB_s = 0 \tag{2.38}$$

κ, the curvature of the layer, is a function only of s and is given in terms of the derivatives of x_L and y_L. The s momentum equation is

$$\rho u\,\partial v/\partial\tilde{n} - \rho v\partial v/\partial s - SvB_n^2 = 0 \tag{2.39}$$

Finally, the energy equation is just the same as (2.1). At the shock, $\tilde{n} = 0$, we have the following boundary conditions (dot indicates d/ds):

$$\rho = 1 \qquad p = \dot{y}_L^2 \qquad u = -\dot{y}_L \qquad v = -\dot{x}_L \tag{2.40}$$

As indicated earlier, we lack general solutions to these equations. Consequently, we resort to a momentum integral method somewhat analogous to that used in boundary-layer theory.[9] We introduce the quantities

$$I(s) = \int v d\tilde{n} \qquad M(s) = \int \rho v d\tilde{n} \qquad P(s) = \int \rho v^2 d\tilde{n} \tag{2.41}$$

These quantities measure, respectively, the current, mass flux, and momentum flux in the deceleration layer. The integrals are carried from the shock $\tilde{n} = 0$ to the effective back of the layer. On integrating (2.38) across the layer, we find

$$\kappa P + p_M - \dot{y}^2 + SB_nB_sI = 0 \tag{2.42}$$

where $p_M(s)$ is the pressure at the back of the deceleration layer. The subscript indicates that we will use this quantity to match with our solution for the flow in the slow flow region. Integrating (2.39) through the layer and making use of the continuity equation (2.36) leads to

$$[\rho uv] - (1/y_L)\int \partial(\rho v^2 y_L)/\partial s\, d\tilde{n} - SB_n^2 I = 0 \tag{2.43}$$

We can evaluate ρuv at the shock using (2.40). At the back

of the layer it is effectively zero since v is reduced to the order of ϵ at that point. Thus,

$$\dot{x}_L\dot{y}_L + (1/y_L)d(Py_L)/ds + SB_n^2I = 0 \qquad (2.44)$$

Rather than evaluate the normal component of velocity at the back of the layer, it is convenient to introduce a stream function appropriate to the layer defined by

$$\rho u = -(1/y_L)\partial(\psi y_L)/\partial s \qquad \rho v = -\partial\psi/\partial\tilde{n} \qquad (2.45)$$

Noting that $\psi = \frac{1}{2}y_L$ at the shock, integration of the second equation (2.45) gives

$$M = \tfrac{1}{2}y_L - \psi_M \qquad (2.46)$$

where ψ_M is the stream function at the back of the shock layer. ψ_M and p_M are the two quantities we use to relate the deceleration layer to the slow flow region.

An interesting observation to make on (2.42) and (2.44) is that, if $S = 0$, corresponding to the aerodynamic case, we can eliminate P directly and find the Busemann relation[10] for the pressure in Newtonian shock layers. When the magnetic interaction is present, no such simple result is available to us. We now have to assume profiles for v and ρ through the layer in terms of a shape parameter $\delta(s)$ of some kind, so that I, M, and P can all be expressed as functions of $\delta(s)$. The problem can then be shown[5] to reduce to a system of five ordinary differential equations for the six unknowns, x_L, y_L, κ, δ, ψ_M, and p_M. To complete the set, we need to introduce one further relation, and this is the slow flow solution (2.27). Along the deceleration layer we have

$$d\eta/ds = (2R/r_s)B_n \sin\phi \qquad (2.47)$$

so that (2.27) becomes

$$\psi_M = -\frac{p_M}{SB_n}\frac{dp_M}{ds}\left[\frac{2R^4}{r_s^3}\frac{\int_0^\phi \sin^{13}t\,dt}{\sin^{14}\phi} + \frac{h(\eta)}{r_sR^3}\right] \qquad (2.48)$$

The equations just described can be used to solve two fundamentally different problems. The first of these, which we call the direct problem (by analogy to a somewhat similar aerodynamic problem), is that in which the body shape and the dipole location relative to the body are given. It is required to find the shape of the shock wave and the deceleration layer. The second problem, which we call the inverse problem, is that in which the shape of the shock wave and deceleration layer are given and also the location of the dipole relative to the shock wave. It is required to find the body shape. We shall give numerical results for both these types of problems subsequently, but before proceeding to these calculations we must consider again our model of the flow in the region away from the stagnation streamline. We have seen how to calculate along the deceleration layer, and we have seen how to join to the deceleration layer a consistent slow flow region. How far can we take this process?

As we proceed along the deceleration layer, p_M falls. Where it reaches zero, the deceleration layer is fully supported by the centrifugal and $j \times B$ forces. Clearly, this point is a natural limit to the validity of our calculation. Another such limit can be found by considering the component of magnetic field normal to the deceleration layer. In all reasonable configurations this field component must drop and will eventually reach zero. We assume that these two points (i.e., the points where p_M and B_n vanish) coincide.

In justification of this model, suppose first that p_M reaches zero while B_n is finite. Equation (2.48) shows that at this point $\psi_M = 0$, that is, the stagnation streamline reaches the deceleration layer at this point. This implies that all the slow flow region is exhausted by being forced back into the deceleration layer. By the definition of the deceleration layer this implies that the slow flow is accelerated at least to sonic velocity in some region near the back of the deceleration layer. But the $j \times B$ force would oppose this acceleration, and therefore, if it exists, it must be due to the pressure gradient. But previously, we saw that, as long as $S\epsilon^{-1/2} \gg 1$, the $j \times B$ force is always greater than the pressure gradient. The argument given there is directly applicable to our case as long as B_n remains of order unity. If B_n is of order $\epsilon^{1/4}$, however, the *effective* interaction parameter makes $S\epsilon^{-1/2} \sim 1$, in which case the pressure gradient does become important. But, on our assumption that $\epsilon^{1/4}$ is small, this implies that B_n is small, which is contrary to our hypothesis. Thus we reject situations in which p_M goes to zero before B_n. The weakest link in the foregoing argument is the assumption $\epsilon^{1/4} \ll 1$. We shall discuss the implications of finite ϵ in Sec. III.

Returning to our model, suppose on the other hand that B_n goes to zero before p_M. From (2.48) we see that, if ψ_M is to remain finite (which is physically essential), either dp_M/ds must vanish or the quantity in brackets must vanish. If dp_M/ds vanishes for finite p_M, p_M goes through a minimum and starts to increase again. This seems to be unrealistic. The quantity in brackets, on the other hand, vanishes at the body and cannot vanish twice on the same field line.

We are, therefore, led (by reductio ad absurdum) to suppose that p_M and B_n vanish simultaneously and that ψ_M is finite at that point. What are the consequences of this model? The numerical answers to this question will be given, but it will be useful to anticipate certain results. At the point where p_M and B_n vanish, the slow flow velocity becomes infinite. This infinity must be regarded as meaning sonic. However, formally speaking, the area required to pass a finite mass at infinite velocity is zero, provided the density is not zero, a condition that is certainly fulfilled for isothermal flow that expands by a factor $e^{1/2}$ in going from stagnation to sonic conditions. Therefore, all the slow flow gas must be immediately behind the point where p_M and B_n go to zero, and the field line through this point delimits the flow in the sense that it must coincide with $\psi = 0$. This point, which has practical importance, will be reviewed in Sec. III in the light of a more realistic view of the gas properties.

We consider now the choice of profiles to be used in calculating I, M, and P. We introduce the following quantities: $\delta(s)$ is an effective thickness of the deceleration layer. ξ, defined by $\xi = \tilde{n}/\delta$, varies from zero at the shock to unity at the back of the layer. We let

$$v/(-\dot{x}_L) = f_1(\xi) \qquad \rho = f_2(\xi) \qquad (2.49)$$

Thus, at the shock we have $f_1(0) = f_2(0) = 1$. At the back of the deceleration layer, v is of order ϵ and thus may be taken to be zero, that is, $f_1(1) = 0$, and from the energy equation (2.44), $f_2(1) = p_M$. These boundary conditions suffice to define linear profiles:

$$f_1(\xi) = 1 - \xi \qquad (2.50)$$

$$f_2(\xi) = 1 - (1 - p_M)\xi \qquad (2.51)$$

With these profiles we readily calculate

$$I(s) = -\dot{x}_L\delta\int_0^1 f_1(\xi)d\xi = -\frac{1}{2}\dot{x}_L\delta \qquad (2.52)$$

$$M(s) = -\dot{x}_L\delta\int_0^1 f_1f_2d\xi = -\frac{1}{6}\dot{x}_L\delta(2 + p_M) \qquad (2.53)$$

$$P(s) = \dot{x}_L^2\delta\int_0^1 f_1^2f_2d\xi = \frac{1}{12}\dot{x}_L^2\delta(3 + p_M) \qquad (2.54)$$

Before we can use these for integration, we must examine their behavior for small s. Since the linear profiles do not agree with the exponential profiles calculated in the deceleration layer analysis, we may expect that the starting conditions developed previously will have to be modified. It can be shown[5] that use of these profiles requires us to replace (2.34) with

$$21S^2 - (32r_s + 18S)[1 - (r_b/r_s)^7] = 0 \qquad (2.55)$$

and that this introduces no substantial errors.

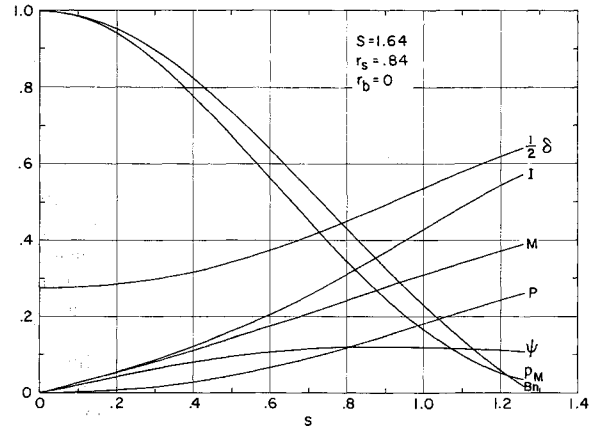

Fig. 6 Variation of the significant quantities relevant to the deceleration layer for the fully magnetohydrodynamic case. The abscissa represents arc length. p_M and B_n vanish at the same place to a sufficient degree of accuracy.

We chose problems characteristic of both the inverse and the direct case for detailed numerical treatment. The inverse problem, finding the shapes of the bodies that go with circular deceleration layers, is treated by Levy et al.[5] and will not be given in detail here. A noteworthy result of this calculation is that, as far as the calculation went, a circular deceleration layer always corresponds to a value of r_s close to 0.7. It is not easy to see why r_s should be as insensitive as it is over this range, but an explanation along the following lines seems reasonable: If $r_s = 1$, $B_n = 0$ at $\theta = \phi = \pi/2$. With centrifugal forces, the deceleration layer can never reach $\theta = \pi/2$ with $p_M > 0$. Therefore, we always expect $r_s < 1$. On the other hand, if B_n is to vanish (i.e., layer and field become parallel) at an angle like one radian, r_s cannot be too small. A second feature to notice is the effect of the seventh power in (2.55). The range of interaction parameters for which r_b/r_s is substantially less than unity is very small. This situation has an important practical consequence. For in some physical situation we could imagine the quantity $\sigma/\rho_\infty u_\infty$ changing by many orders of magnitude. The significance of the seventh power in (2.55) is then that the change from quasi-aerodynamic to fully magnetohydrodynamic flow takes place when $\sigma/\rho_\infty u_\infty$ varies only by a factor of 2 or so. Put another way, the fully magnetohydrodynamic case is either "on" or "off" in any physical situation.

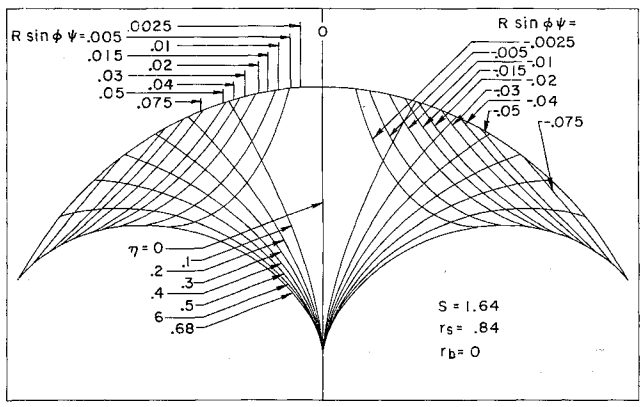

Fig. 7 Representation of the streamlines for the fully magnetohydrodynamic flow. Equal masses flow between the streamlines shown. Note the displacement of the streamlines in the deceleration layer. The magnetic field lines are also shown. The center of curvature of the shock is at the bottom of the figure.

We turn now to a direct problem, finding the deceleration layer that goes with no body. In this case the geometry is initially unknown. With $r_b = 0$, (2.55) is a relation between S and r_s; it is a question of finding which pair of values S and r_s, satisfying (2.55), leads [using $h(\eta) \equiv 0$] to a deceleration layer for which p_M and B_n vanish simultaneously. The result of the calculation was $S = 1.64$, $r_s = 0.84$. The variation of the properties along the deceleration layer are shown in terms of arc length in Fig. 6, and the slow flow region and over-all geometry are shown in Fig. 7. The resultant shock shape is, as can be seen, nearly circular. The limiting streamline is the field line $\eta = 0.68$. The most important number to emerge from this analysis is the value $S = 1.6$, for this is the largest possible value of S; any further increase in, say, the conductivity or magnetic moment of the coil, results only in a larger standoff distance, the value of S being unchanged. Figure 7 should probably be disregarded beyond about $\eta = 0.5$, on which field line the pressure and density are about 0.25. Beyond this field line, Fig. 7 predicts a substantial rise in velocity (coming together of the streamlines) indicating that the low Mach number approximation is no longer valid.

III. Discussion and Conclusions

The principal result of the foregoing analysis is that when

$$S = \epsilon\sigma u_\infty r_c B_0^2/\rho_\infty u_\infty^2 \approx 1.6 \qquad (3.1)$$

a flow pattern is set up in which the forces acting on the flow are almost entirely magnetic in origin. Forces exerted at solid surfaces are important only over a negligible area around the stagnation point. The demonstration that this type of flow can exist even at low magnetic Reynolds number was one of our principal objectives. On the other hand, the result (3.1) was not achieved without making a number of assumptions, nearly all of which need closer examination if we are to make a more accurate assessment of the physical conditions to which (3.1) should apply. In this section we shall discuss some of these physical conditions and also mention briefly the situation as regards experimental (laboratory) verification of the theoretical work in this area.

We commence with a discussion of the effects of finite (as opposed to vanishingly small) ϵ. In practical situations ϵ may be as small as 0.05, in which case $\epsilon^{1/4}$ is about 0.5. This obviously casts a shadow on those parts of the flow picture dependent on $\epsilon^{1/4}$ being small, notably the joining of the deceleration layer to the slow flow region near the sonic points. We feel, however, that the effect of finite ϵ will be one in which things get "smeared out" rather than fundamentally changed. Most notably, for finite ϵ, the slow flow will require a considerable area to be passed out at sonic speed parallel to the magnetic field. However, the distinction between the deceleration layer and the slow flow region is also less distinct for larger ϵ, so that it seems fair to describe the net effect as one "blurring" a picture whose sharp outlines are useful for descriptive and mathematical purposes, but not physically realistic.

We turn next to consideration of the Hall effect. When $\omega\tau$ is not small, the electric current is reduced in magnitude and does not flow in the direction of the applied electric field. However, cases can arise in which the angle between the current and the electric field remains small, and the magnitude of the current stays the same even though $\omega\tau$ grows to values in excess of unity. Just such a case arose in the paper of Levy and Petschek.[4] Here the Hall currents (roughly the component of the electric current perpendicular to the electric field) were restricted to flow in a long narrow region of aspect ratio ϵ. This inhibited them to the extent that no important effect was noted until $\omega\tau$ grew to values in excess of ϵ^{-1}. This case does not occur in the present geometry; the Hall currents would flow, in this case, throughout the slow flow region. For this reason, the result (3.1)

can be expected to hold only for values of $\omega\tau$ less than unity. Toward the edge of the slow flow region $\omega\tau$ will rise considerably because of the decrease in the gas density. Thus the Hall effect will limit the sharpness of the boundary to the slow flow region. A similar effect is ion slip, which occurs when the density is so low that the neutrals can leak past the ions. The presence of ion slip would result in some small heat transfer to those parts of the surface of the body which the ideal theory shows to be not in contact with the hot gas.

A further physical limitation is that of chemical nonequilibrium. At sufficiently low density there may not be time for the ionization processes in the gas to reach equilibrium. Thus Boyer[11] claims that nonequilibrium effects make the attainment of substantial interaction parameters in hypersonic wind-tunnel facilities problematical for unseeded air. For the flight case, it is probably fair to say that, where nonequilibrium effects are important, the density must be so low as to preclude useful dynamic effects. However, it is difficult to generalize on this subject, and we must usually be content with calculating the magnitude of likely effects in any given case.

A final limitation on the physical realizability of the flows discussed in this paper arises from the following considerations. The gas ahead of the strong shock is supposed to be cold and un-ionized, a condition that is certainly met in the planetary entry case. However, the magnetic field of the coil extends substantially beyond the shock, and the cold gas therefore "sees" an effective electric field. The question arises as to whether this electric field is sufficient to break down the gas. This question is quite involved and is discussed at the end of the paper by Levy and Petschek.[4] On the one hand, arguments can be given to show that breakdown could not occur for velocities less than about 5×10^6 cm/sec, i.e., about five times satellite velocity. On the other hand, unanswered questions remain having to do with the possibility of substantial photo ionization in the gas ahead of the shock.

This comment about photo ionization introduces the subject of radiant heat transfer. It has been shown, for instance, by Goulard[12] and Romig[13]§ that the magnetohydrodynamic interaction can sometimes increase the radiant heat transfer to a body while decreasing the convective heat transfer, the flow conditions remaining fixed. This effect is due to the increased volume of hot radiating gas that is a consequence of the increase in the standoff distance. Since in this paper we deal only with the dynamics of the flow, and since under ordinary conditions radiation does not affect the dynamics of this type of flow, we shall not pursue this subject here. It does seem worth pointing out however, that, for a fixed object, re-entry may take place at a higher altitude because of dynamic effects. Thus, the radiant heat transfer to a body could be reduced by causing it to decelerate at a higher altitude.

We conclude by reviewing the status of quantitative experiment in the field of low magnetic Reynolds number hypersonic flows. Early work in the field by Bush and Ziemer[14] appeared to give good results, but a recent article by Cloupeau[15] appears to throw some doubt on the quantitative interpretation of results achieved in electromagnetic shock tubes of the type used by Bush and Ziemer. Work on this subject has also been reported by Wilkinson[16] and Ericson et al.,[17] although neither of these studies appears to have given very good results. We understand that a description by Locke, Petschek, and Rose[18] of experimental work performed by them with the object of verifying the existence of fully magnetohydrodynamically supported hypersonic flows (as predicted by Levy and Petschek[4]) is forthcoming. Preliminary results indicate that such flows can be supported with negligible physical contact between the hot gas and solid surfaces.

§ We are indebted to a reviewer for this reference.

References

[1] Kemp, N. H., "On hypersonic stagnation point flow with a magnetic field," J. Aeronaut. Sci. **25**, 405–407 (1958); also Freeman, N. C., "On the flow past asphere at hypersonic speed; with a magnetic field," J. Aerospace Sci. **26**, 670–672 (1959) also Kemp, N. H., "Author's reply," J. Aerospace Sci. **26**, 672 (1959).

[2] Bush, W. B., "Magnetohydrodynamic-hypersonic flow past a blunt nose," J. Aerospace Sci. **25**, 685–690 (1958); also Bush, W. B., "A note on magnetohydrodynamic-hypersonic flow past a blunt body," J. Aerospace Sci. **26**, 536 (1959).

[3] Lykoudis, P. S., "The Newtonian approximation in magnetic hypersonic stagnation-point flow," J. Aerospace Sci. **28**, 541–546 (1961).

[4] Levy, R. H. and Petschek, H. E., "Magnetohydrodynamically supported hypersonic shock layer," Phys. Fluids **6**, 946–961 (1963).

[5] Levy, R. H., Gierasch, P. J., and Henderson, D. B., "Hypersonic magnetohydrodynamics with or without a blunt body," Avco-Everett Research Lab. Research Rept. 173 (January 1964).

[6] Kemp, N. H. and Petschek, H. E., "Two-dimensional incompressible magnetohydrodynamic flow across an elliptical solenoid," J. Fluid Mech. **4**, 553 (1958).

[7] Hains, F. D., Yoler, Y. A., and Ehlers, E., "Axially symmetric hydromagnetic channel flow," *Dynamics of Conducting Gases*, edited by A. B. Cambel and J. B. Fenn (Northwestern University Press, Evanston, Ill., 1959), pp. 86–103.

[8] Li, T. Y. and Geiger, R. E., "Stagnation point of a blunt body in hypersonic flow," J. Aeronaut. Sci. **24**, 25 (1957).

[9] Pohlhausen, K., "Zur naherungsweisen Integration der Differentialgleichung der laminaren Reibungsschicht," Z. Angew. Math. Mech. **1**, 252 (1921).

[10] Busemann, A., "Flussigkeits-und-Gasbewegung," *Handworterbuch der Naturwissenschaften* (VEB Gustav Fischer, Verlag, Jena, 1933), 2nd ed., Vol. IV, pp. 244–279.

[11] Boyer, D. W., "Ionization nonequilibrium effects on the magnetogasdynamic interaction in the stagnation region of an axisymmetric blunt body," Cornell Aeronautical Lab. Rept. AG-1547-Y-1 (June 1963).

[12] Goulard, R., "An optimum magnetic field for stagnation heat transfer reduction at hypersonic velocities," ARS J. **29**, 604 (1959).

[13] Romig, M. F., "The influence of electric and magnetic fields on heat transfer to electrically conducting fluids," *Advances in Heat Transfer* (Academic Press, New York, 1964), Vol. 1.

[14] Bush, W. B. and Ziemer, R. W., "Magnetic field effects on bow shock stand-off distance," Phys. Rev. Letters **1**, 58 (1958).

[15] Cloupeau, M., "Interpretation of luminous phenomena observed in electromagnetic shock tubes," Phys. Fluids **6**, 679–688 (1963).

[16] Wilkinson, J. B., "Magnetohydrodynamic effects on stagnation-point heat transfer from partially ionized nonequilibrium gases in supersonic flow," AeroChem TP-43, AeroChem Research Lab., Inc., Princeton, N. J. (March 1962).

[17] Ericson, W. B., Maciulaitis, A., Spagnolo, R. A., Loeffler, A. L., Scheuing, R. A., Hopkins, H. B., "An investigation of magnetohydrodynamic flight control," Grumman Aircraft Engineering Corp., Bethpage, N. Y. (May 1962).

[18] Locke, E. V., Petschek, H. E., and Rose, P. H., "Experiments with magnetohydrodynamically-supported shock layers," Avco-Everett Research Lab., Research Rept. 191 (August 1964); also Phys. Fluids (to be published).